JACS
JOURNAL OF THE AMERICAN CHEMICAL SOCIETY
Article
pubs.acs.org/JACS

Self-Assembly and Photocatalytic Properties of Polyoxoniobates: $\{Nb_{24}O_{72}\}$, $\{Nb_{32}O_{96}\}$, and $\{K_{12}Nb_{96}O_{288}\}$ Clusters

Peng Huang, Chao Qin, Zhong-Min Su,* Yan Xing, Xin-Long Wang,* Kui-Zhan Shao, Ya-Qian Lan, and En-Bo Wang*

Institute of Functional Materials Chemistry, Key Laboratory of Polyoxometalate Science of Ministry of Education, Department of Chemistry, Northeast Normal University, Changchun 130024, People's Republic of China

Supporting Information

ABSTRACT: Three novel polyoxoniobates, $KNa_2[Nb_{24}O_{72}H_{21}]\cdot 38H_2O$ (**1**), $K_2Na_2[Nb_{32}O_{96}H_{28}]\cdot 80H_2O$ (**2**), and $K_{12}[Nb_{24}O_{72}H_{21}]_4\cdot 107H_2O$ (**3**) with molecular triangle, molecular square, and cuboctahedral molecular cage geometries, respectively, have been successfully synthesized by conventional aqueous methods. All the compounds are built from $[Nb_7O_{22}]^{9-}$ fundamental building units. Compound **1** is the first isolated $\{Nb_{24}O_{72}\}$ cluster, featuring three heptaniobate clusters linked in a ring by three additional NbO_6 octahedra, while compound **2** is the largest isopolyoxoniobate cluster reported to date, consisting of four heptaniobate clusters linked by four additional NbO_6 octahedra. Compound **3** is the largest solid aggregation of polyoxoniobates, assembled by four $\{KNb_{24}O_{72}\}$ clusters joined by four K ions. To our knowledge, it is the first time these polyoxoniobate clusters have been crystallized with only alkali-metal counterions, thereby giving them the possibility of being redissolved in water. ESI-MS spectra indicate that compounds **1** and **2** remain structural integrity when the pure, crystalline polyanion salts are dissolved in water, while compound **3** is partially assembled into Nb_{24} fragments. The UV–vis diffuse reflectance spectra of these powder samples indicate that the corresponding well-defined optical absorption associated with E_g can be assessed at 3.35, 3.17, and 3.34 eV, respectively, revealing the presence of an optical band gap and the nature of semiconductivity with a wide band gap. UV-light photocatalytic H_2 evolution activities were observed for these compounds with $Co^{III}(dmgH)_2pyCl$ as a cocatalyst and TEA as a sacrificial electron donor.

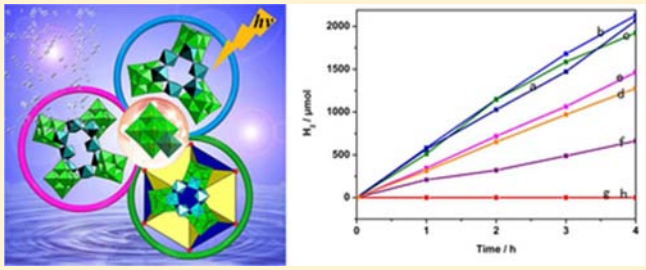

INTRODUCTION

Polyoxometalates (POMs) are attractive transition-metal oxide nanoclusters, owing to their unmatched physical and chemical properties, and have held great promise for a variety of applications in catalysis, medicine, materials science, and nanotechnology.[1] Currently, using POM building blocks to construct larger clusters has given rise to significant interest. Some achievements in this aspect have been made with persistent efforts. For example, some exceptionally large ring-shaped oxomolybdenum clusters that contain up to several hundred metal centers have been reported.[2] To date, the development of POM chemistry is still focused on the polyoxotungstates, polyoxomolybdates, and polyoxovanadates because they can be easily obtained with simple acidification and are stable over a wide pH range.[3] Polyoxoniobates (PONbs), as a burgeoning subclass, have attracted increasing interest because of their unique characteristics (high charge/surface ratio and basicity) and potential applications in nuclear-waste treatment and virology.[4] The perspective paper of Nyman "Polyoxoniobate Chemistry in the 21st Century" summarizes the recent successes, continuing shortcomings, and some unique and potentially exploitable features of PONb chemistry.[4f] At present, the development of PONbs is still at its early stage, owing to the difficulty of controlling synthetic conditions such as the narrow pH range and the lack of the building unit that has been dominated by the isopolyoxoniobate $[Nb_6O_{19}]^{8-}$.[5] In 1977, the decaniobate ion $[Nb_{10}O_{28}]^{6-}$ was determined by Graeber and Morosin.[6] In 2002, Nyman's group synthesized the Keggin-type heteropolyniobate cluster $\{[Ti_2O_2][SiNb_{12}O_{40}]\}^{12-}$ and the lacunary derivative $[H_2Si_4Nb_{16}O_{56}]^{14-}$ under hydrothermal conditions.[7] Subsequently, the series of Keggin-based dodecaniobates $[XNb_{12}O_{40}]^{16-}$, $[Ti_2O_2][XNb_{12}O_{40}]^{12-}$, $[Nb_2O_2][XNb_{12}O_{40}]^{10-}$, and $[SiNb_{18}O_{54}]^{14-}$ were reported (X = Si^{IV}, Ge^{IV}).[8] In 2006, Yagasaki et al. prepared the icosaniobate $[Nb_{20}O_{54}]^{8-}$.[9] Recently, Cronin's group obtained the two huge polyoxoniobates $[HNb_{27}O_{76}]^{16-}$ and $[H_{10}Nb_{31}O_{93}(CO_3)]^{23-}$ built from pentagonal $\{Nb(Nb)_5\}$ units.[10] Although PONb chemistry has made some progress in the synthesis and characterization of novel compounds, a systematic synthetic strategy and property investigation remain less developed.

Although a study of the photocatalytic H_2 evolution activity of the polyoxotungstates has been carried out several years before,[11] the photocatalytic activity research of PONbs is still in its infancy. Osterloh discussed some inorganic materials as

Received: April 20, 2012
Published: August 20, 2012

dx.doi.org/10.1021/ja303723u | J. Am. Chem. Soc. 2012, 134, 14004–14010

catalysts for photochemical splitting of water in his excellent review, therein including the niobates and tantalates.[12] Very recently, Feng et al. demonstrated the photocatalytic water-splitting activity of the heteropolyoxoniobate $K_{10}[Nb_2O_2(H_2O)_2][SiNb_{12}O_{40}]\cdot 12H_2O$.[13] We thus believe that PONbs would be good candidates for photocatalysis.

The first structurally characterized isopolyoxoniobate was the Lindqvist-type anion $[Nb_6O_{19}]^{8-}$, which acts as a cornerstone for the advancement of PONb chemistry.[14] The large isopolyanionic $[H_9Nb_{24}O_{72}]^{15-}$ building unit has been reported by Nyman and Niu on the basis of $[Nb_7O_{22}]^{9-}$ building units, which is a triangular "bowl-shaped" cluster with C_{3v} point symmetry.[15] Inspired by the aforementioned work, we are aware that the $[Nb_7O_{22}]^{9-}$ subunit might be a good candidate for the construction of larger polyniobate aggregates. Herein we report the syntheses, structures, and photocatalytic properties of three $[Nb_7O_{22}]^{9-}$-based isopolyoxoniobates, $KNa_2[Nb_{24}O_{72}H_{21}]\cdot 38H_2O$ (**1**), $K_2Na_2[Nb_{32}O_{96}H_{28}]\cdot 80H_2O$ (**2**), and $K_{12}[Nb_{24}O_{72}H_{21}]_4\cdot 107H_2O$ (**3**). The reaction stoichiometries for these materials are as follows:

$$2NaOH(s) + 4K_7HNb_6O_{19}\cdot 13H_2O(s) + 7H_2O = KNa_2[Nb_{24}O_{72}H_{21}]\cdot 38H_2O(s) + 27KOH$$

$$6NaOH(s) + 16K_7HNb_6O_{19}\cdot 13H_2O(s) + 116H_2O = 3K_2Na_2[Nb_{32}O_{96}H_{28}]\cdot 80H_2O(s) + 106KOH$$

$$16K_7HNb_6O_{19}\cdot 13H_2O(s) = K_{12}[Nb_{24}O_{72}H_{21}]_4\cdot 107H_2O(s) + 100KOH + 17H_2O$$

Compound **1** is the first isolated molecular triangle $\{Nb_{24}O_{72}\}$ cluster, which is assembled into a 1D nanotube with a diameter of 30.6 Å, while compound **2** contains the molecular square $\{Nb_{32}O_{96}\}$ cluster, which is the largest isopolyoxoniobate cluster to date. Compound **3** is the largest solid aggregation of PONbs with cuboctahedral geometry. The phase purity of the products was confirmed by the agreement between the experimental X-ray powder diffraction (XRPD) patterns and the simulated patterns based on structure analysis (Figures S1–S3, Supporting Information).

EXPERIMENTAL SECTION

Materials. All reagents and solvents for the syntheses were purchased from commercial sources and used as received, except for $K_7HNb_6O_{19}\cdot 13H_2O$ and $Co^{III}(dmgH)_2pyCl$ (the structure is shown in Scheme S1 (Supporting Information)), which were synthesized according to the literature[16] and characterized by IR spectra and elemental analysis. $KTaO_3$ was purchased from Alfa and used without further purification.

Instruments. The Fourier transform infrared spectroscopy (FTIR) spectra were recorded from KBr pellets in the range 4000–300 cm^{-1} on a Mattson Alpha-Centauri spectrometer. PXRD patterns were recorded on a Siemens D5005 diffractometer with Cu Kα (λ = 1.5418 Å) radiation in the range 3–50°. Elemental analyses (C, H, and N) were measured on a Perkin-Elmer 2400 CHN elemental analyzer; Nb, K, and Na were determined with a Plasma-SPEC(I) ICP atomic emission spectrometer. UV–vis absorption spectroscopy was obtained on a U-3010 spectrophotometer (Hitachi, Japan). Thermogravimetric analyses (TGA) were performed on a Perkin-Elmer TGA 7 analyzer heated from room temperature to 1000 °C under a nitrogen gas atmosphere with a heating rate of 10 °C min^{-1}. Electrospray ionization mass spectrometry was carried out with a Bruker Micro TOF-QII instrument.

Synthesis and Characterization of 1. 1,4-Diaminobutane (0.176 g, 2 mmol) was added to a solution of $Cu(OAc)_2\cdot H_2O$ (0.2 g, 1.0 mmol) in water (10 mL) with stirring. Then the resulting purple solution was added dropwise to a solution of $K_7HNb_6O_{19}\cdot 13H_2O$ (0.685 g, 0.5 mmol) in water (50 mL) with stirring in a 100 mL beaker. Subsequently, the mixture was adjusted to pH 10.5–11.2 using NaOH (1 mol L^{-1}) solution, condensed to 35 mL at 50–60 °C for 5 h, filtered, and then transferred to a 50 mL beaker. Two days later, the blue precipitate that formed was filtered off. The colorless filtrate was transferred to a 50 mL open beaker again and was allowed to evaporate slowly under ambient temperature (room temperature about 15 °C). After 3 weeks, colorless crystals were obtained. Yield: 0.3 g (57.53% based on $K_7HNb_6O_{19}\cdot 13H_2O$). Anal. Calcd: Nb, 53.44; K, 0.94; Na, 1.10. Found: Nb, 53.86; K, 0.89; Na, 1.28. IR (KBr disks): 843, 772, 688, 537 cm^{-1}.

Synthesis and Characterization of 2. Isonicotinic acid (0.246 g, 2 mmol) was added to a stirred solution of $Cu(OAc)_2\cdot H_2O$ (0.2 g, 1.0 mmol) dissolved in 20 mL of water. Then, the blue solution was added to a stirred aqueous solution (50 mL) containing $K_7HNb_6O_{19}\cdot 13H_2O$ (0.685 g, 0.5 mmol). The resulting cloudy solution was adjusted to pH 10.6–11.5 using NaOH (1 mol L^{-1}) solution at 55–60 °C and then was filtered quickly to give a colorless solution. The filtrate was allowed to evaporate slowly at ambient temperature in an open 100 mL beaker (room temperature about 15 °C). Over a period of 4 weeks, colorless block single crystals for X-ray crystallography were obtained and air-dried to give 0.23 g of **2** (41% yield based on $K_7HNb_6O_{19}\cdot 13H_2O$). Anal. Calcd: Nb, 48.72; K, 1.28; Na, 0.75. Found: Nb, 48.47; K, 1.13; Na, 0.84. IR (KBr disks): 873, 771, 677, 529 cm^{-1}.

Synthesis and Characterization of 3. A 10% acetic acid solution was added dropwise to a stirred solution of $K_7HNb_6O_{19}\cdot 13H_2O$ (0.685 g, 0.5 mmol) dissolved in 50 mL of water, until the pH of the solution was adjusted to 9. Then, 1,3-diaminopropane (0.148 g, 2 mmol) was added dropwise to the stirred aqueous solution. Subsequently, the mixture was adjusted to pH 10–11.5 using NaOH (1 mol L^{-1}) solution, condensed to 35 mL at 50–60 °C for 5 h, filtered, and then transferred to a 50 mL beaker. The filtrate was allowed to evaporate slowly at ambient temperature (room temperature about 15 °C). Over a period of 3 weeks, colorless block single crystals for X-ray crystallography were obtained, washed with cold water, and air-dried to give 0.29 g of **3** (58% yield based on $K_7HNb_6O_{19}\cdot 13H_2O$). Anal. Calcd: Nb, 55.71; K, 2.93. Found: Nb, 55.45; K, 3.28. IR (KBr disks): 888, 651 cm^{-1}.

Single-Crystal Studies. Single-crystal X-ray diffraction data for **1**–**3** were recorded on a Bruker Apex CCD II area-detector diffractometer with graphite-monochromated Mo Kα radiation (λ = 0.710 73 Å) at 293 K. Absorption corrections were applied using multiscan techniques. Their structures were solved by direct methods of SHELXS-97 and refined by full-matrix least-squares techniques using the SHELXL-97 program.[17] Anisotropic thermal parameters were used to refine all non-hydrogen atoms, with the exception of some oxygen atoms. Hydrogen atoms attached to lattice water molecules were not located. Crystallization water molecules were estimated by thermogravimetry, and only partial oxygen atoms of water molecules were achieved with the X-ray structure analysis. **1**: $H_{97}KNa_2Nb_{24}O_{110}$, M_r = 4172.7, trigonal, $P6_3/m$, $a = b$ = 29.688(5) Å, c = 30.488(5) Å, γ = 120(5)°, V = 23271(7) Å^3, Z = 6, ρ_{calcd} = 1.786 g cm^{-3}, final R1 = 0.0435 and wR2 = 0.1223 (R_{int} = 0.0620 after SQUEEZE) for 13 927 independent reflections ($I > 2\sigma(I)$). **2**: $H_{188}K_2Na_2Nb_{32}O_{176}$, M_r = 6102.80, triclinic, $P\bar{1}$, a = 12.844(5) Å, b = 17.578(5) Å, c = 19.973(5) Å, α = 84.513(5)°, β = 73.271(5)°, γ = 81.818(5)°, V = 4267(2) Å^3, Z = 1, ρ_{calcd} = 2.301 g cm^{-3}, final R1 = 0.0480 and wR2 = 0.1147 (R_{int} = 0.0387 after SQUEEZE) for 14 738 independent reflections ($I > 2\sigma(I)$). **3**: $H_{298}K_{12}Nb_{96}O_{395}$, M_r = 16 008.95, trigonal, $R\bar{3}$, $a = b$ = 39.2527(14) Å, c = 106.905(7) Å, γ = 120°, V = 142648(12) Å^3, Z = 6, ρ_{calcd} = 2.233 g cm^{-3}, final $R1$ = 0.0560 and wR2 = 0.0921 (R_{int} = 0.1529 after SQUEEZE) for 33 175 independent reflections ($I > 2\sigma(I)$). CCDC 861116 (**1**), 861114 (**2**),

and 861115 (**3**) contain supplementary crystallographic data for this paper. These data can be obtained free of charge from the Cambrige Crystallographic Data Centre via www.ccdc.cam.ac.uk/data_request/cif for **1**−**3**.

Photocatalytic Measurements. Photocatalytic reactions were carried out in a Pyrex inner-irradiation-type reaction vessel with a magnetic stirrer at room temperature. The reactant solution was evacuated using N_2 several times to ensure complete air removal and then irradiated by using a 500 W mercury lamp. The produced H_2 was analyzed by a GC9800 instrument with a thermal conductivity detector and a 5 Å molecular sieve column (2 mm × 2 m) using N_2 as carrier gas.

RESULTS AND DISCUSSION

Synthesis. As mentioned above, the $[Nb_7O_{22}]^{9-}$ ion is a good candidate for the construction of larger polyniobate aggregates. Unfortunately, it only exists in the form of an intermediate. Therefore, a probe into the synthetic conditions favorable for the existence of heptaniobate is of great significance, by which polyoxoniobate chemistry can be further expanded. Breakdown of the hexaniobate to provide monomers and their subsequent reassembly into the heptaniobate has proved to be a promising pathway. The previous work indicates that niobate clusters based on the heptaniobate unit can be obtained between around pH 9−11.[15] Thus, we carried out all the parallel experiments in the pH range 9.5−12.5, with an interval of 0.1. The results indicate that the optimal pH ranges for the isolation of **1**−**3** are 10.5−11.2, 10.6−11.5, and 10−11.5, respectively. This reinforces the fact that the optimal pH range for the existence of heptaniobate is 9.5−11.5. In the synthesis of **1**, we also tried to use different kinds of amines (1,3-diaminopropane, 1,2-diaminopropane, ethylenediamine, diethylenetriamine) to replace 1,4-diaminobutane, but the results proved unsuccessful. Meanwhile, we found that the experimental phenomena are different when those amines with sizes smaller than that of 1,4-diaminobutane (1,3-diaminopropane, 1,2-diaminopropane, ethylenediamine, diethylenetriamine) were used, and the reaction solutions adding them were clear throughout the whole process, in contrast to the large amount of precipitate in the presence of 1,4-diaminobutane. Likewise, when isonicotinic acid was replaced by other different amines, compound **2** was not obtained. Considering that the copper ion was not involved in the resulting structures of **1** and **2**, we removed it in the preparation procedures; however, the experimental results demonstrate that compounds **1** and **2** cannot be obtained. We thus speculate that the roles of $Cu(OAc)_2{\cdot}H_2O$ as well as of longer amines or isonicotinic acid are likely in the formation of precipitates with $K_7HNb_6O_{19}{\cdot}13H_2O$ beforehand, as observed in the preparation procedures of **1** and **2**. With the generation of precipitates, large quantities of copper ions and organic ligands are pulled out of the solution, and as a result, the filtrate is colorless. The lack of copper ions and organic ligands in solution might result in the crystallization of these large niobate clusters without the use of copper amine counteractions but only with alkali-metal counterions—which means these clusters have the possibility of being redissolved in water. In our further work, we will explore the applicability of this synthetic strategy so as to provide general insights into polyoxoniobate syntheses. In comparison with the extreme conditions required in the synthesis of the former two compounds, the synthetic conditions of **3** are relatively insensitive. We found that as long as the reaction pH values are kept in the range 10−11.5, compound **3** can be obtained without considering the kinds of amines used. We have used 1,2-diaminopropane, 1,4-diaminobutane, diethylenetriamine, triethylenetetramine, and tetraethylenepentamine to replace 1,3-diaminopropane, and the results proved that the yield is the highest (about 58%) in the case of 1,3-diaminopropane. The yields are about 30−40% in the presence of other amines. The summary of parallel experiments is given in Table S1 (Supporting Information). In addition, the following do's and don'ts are very important for ensuring the experimental reproducibility. In the synthetic procedure of **2**, when the cloudy solution was adjusted to pH 10.6−11.5 using NaOH solution, it must be filtered quickly. Otherwise, a blue-green filtrate will be obtained, slow evaporation from which will produce the green crystals reported by Niu et al. (CSD 417652).[15b] As shown in the above syntheses, these "spectator" ligands are necessary for the formation of compounds **1**−**3**, although we are unable to propose a definite explanation as to their roles at present.

Structure Description of 1−3. X-ray structural analyses indicate that compounds **1**−**3** are all constructed from the fundamental building unit $[Nb_7O_{22}]^{9-}$. The $[Nb_7O_{22}]^{9-}$ subunit is a derivant of the Lindqvist-type hexaniobate anion $[Nb_6O_{19}]^{8-}$, the three adjacent μ_2-oxygen atoms of which are bonded to the seventh Nb atom, Nb(7) (Figure S4, Supporting Information). Interestingly, the $Nb(7)O_6$ octahedron in the $[Nb_7O_{22}]^{9-}$ fragment has three terminal oxygen atoms with higher coordination ability than the other six NbO_6 octahedra, which provides a necessary condition for constructing the architectures of compounds **1**−**3**. There are four types of O atoms in the $[Nb_7O_{22}]^{9-}$ polyanion: nine terminal oxygen atoms (O_t), nine bridging μ_2-oxygen atoms, three bridging μ_3-oxygen atoms, and one μ_6-oxygen atom in the center. The Nb−O bond lengths range from 1.737(3) to 2.475(3) Å, and the Nb···Nb distances are in the range 3.209(3)−3.394(3) Å.

Compound **1** crystallizes in the trigonal space group $P6_3/m$. There is a half isolated $[Nb_{24}O_{72}H_{21}]^{3-}$ cluster in the asymmetric unit (Figure 1b). The isolated $[Nb_{24}O_{72}H_{21}]$ cluster is composed of three $[Nb_7O_{22}]^{9-}$ cores and three NbO_6 octahedra, where three additional NbO_6 octahedra plus three niobate octahedra outside the hexaniobate units comprise

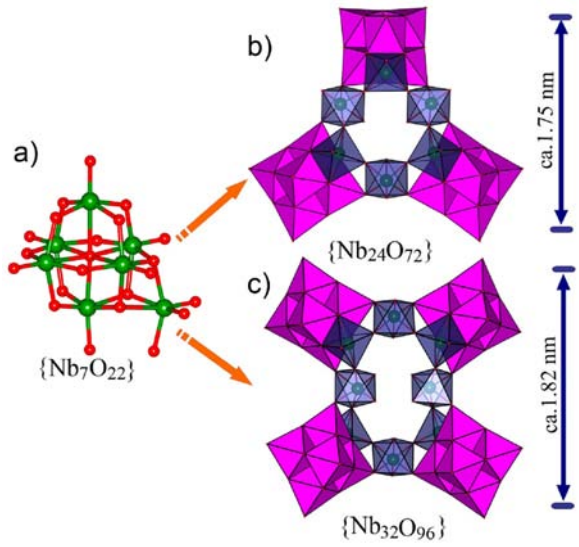

Figure 1. (a) $\{Nb_7O_{22}\}$ building unit. (b) Polyhedral view of the $\{Nb_{24}O_{72}\}$ cluster of **1**. (c) Polyhedral view of the $\{Nb_{32}O_{96}\}$ cluster of **2**.

a six-membered ring (Figures S5 and S6, Supporting Information). Although the $\{Nb_{24}O_{72}\}$ clusters coordinated with other motifs have been observed in the hybrids before,[15] the isolated cluster has never been found to date. Interestingly, the 3D supramolecular network of **1** forms a 1D nanotube along the crystallographic *c* axis with efficient inner and exterior diameters of 14.8 and 30.6 Å, respectively (Figure S7, Supporting Information). First, six $\{Nb_{24}O_{72}\}$ units form a macrocyclic building unit parallel with the crystallographic *ab* plane. Then, the adjacent macrocyclic building units are further packed into a 1D nanotubular structure via hydrogen-bonding interactions. Finally, such nanotubes extend into an unprecedented 3D architecture (Figure 2).

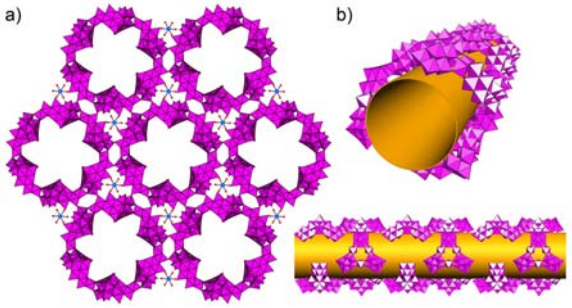

Figure 2. (a) 2D snowflake-like tunnel architecture built by $\{Nb_{24}O_{72}\}$ units in **1**. (b) Perspective view of a tunnel.

Compound **2** contains the $[Nb_{32}O_{96}H_{28}]^{4-}$ cluster with molecular square geometry. The $[Nb_{32}O_{96}H_{28}]^{4-}$ cluster is composed of four $[Nb_7O_{22}]^{9-}$ cores and four NbO_6 octahedra, where four additional NbO_6 octahedra plus four niobate octahedra outside the hexaniobate units comprise an eight-membered ring. As a result, this large isopolyoxoniobate cluster $\{Nb_{32}O_{96}H_{28}\}$ can also be depicted as 4 Lindqvist $\{Nb_6O_{19}\}$ clusters linked together by a cyclic $\{Nb_8O_{40}\}$ fragment (Figure 1c). There are four types of O atoms in the $\{Nb_{32}O_{96}\}$ polyanion: namely, 28 terminal oxygen atoms (O_t), 52 bridging μ_2-oxygen atoms, 12 bridging μ_3-oxygen atoms, and 4 μ_6-oxygen atoms. The Nb−O_t, Nb−μ_2-O, Nb−μ_3-O, and Nb−μ_6-O bond lengths in $\{Nb_{32}O_{96}\}$ cluster range from 1.752(14) to 2.431(12) Å, from 1.839(12) to 2.237(12) Å, from 2.008(11) to 2.267(12) Å, and from 2.270(13) to 2.451(13) Å, respectively, and the Nb···Nb distances are in the range 3.273(2)−3.359(3) Å. As far as we know, prior to this work, the largest isopolyoxoniobate has been $[HNb_{27}O_{76}]^{16-}$, reported by Cronin et al. in 2010.[10] Therefore, the $[Nb_{32}O_{96}H_{28}]^{4-}$ anion reported herein represents the largest isopolyoxoniobate cluster so far discovered.

Compound **3**, $[K_8\{KNb_{24}O_{72}H_{21}\}_4]$, contains the fundamental building block $\{Nb_{24}O_{72}\}$ cluster, which is shown in Figure 3a. Single-crystal X-ray analysis reveals that **3** crystallizes in the trigonal space group $R\bar{3}$ with a large cell volume of 142 648 Å^3 and exhibits a cuboctahedral molecular cage constructed from four $\{KNb_{24}O_{72}\}$ units and four K ions (Figure 3b). Each $\{KNb_{24}O_{72}\}$ unit connects with three K^+ ions, while each K^+ ion links with three different $\{Nb_{24}O_{72}\}$ clusters (K−O = 2.637(3)−2.837(3) Å). Thus, each $\{KNb_{24}O_{72}\}$ unit acts as a triangular three-connected SUB. Furthermore, the most intriguing feature is that four $\{KNb_{24}O_{72}\}$ SUBs are joined together by four K ions to form a large cuboctahedral molecular cage with an inner diameter of approximately 1.2 nm and an

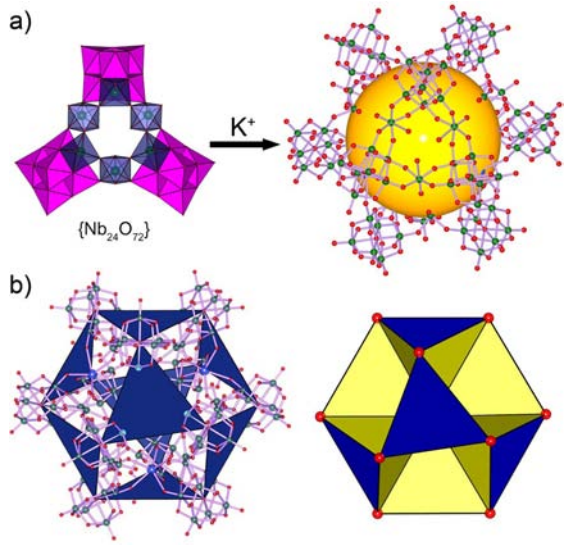

Figure 3. (a) Polyhedral view of the $\{Nb_{24}O_{72}\}$ cluster and a ball-and-stick plot of the molecular cage of **3**. (b) Archimedean polyhedra of compound **3**.

external diameter of about 2.66 nm. The effective free volume calculated by PLATON corresponds to ca. 30.7% of the cell volume (43 778 Å^3 out of the 142 648 Å^3) in which lattice water molecules are located.[18] The 3D packing diagram of **3** along the *c* axis shows a hexagonal close-packed structure (Figure S8, Supporting Information). To our knowledge, compound **3** is the largest solid aggregation of polyoxoniobate with cuboctahedral geometry.

Charge-balance considerations of **1**−**3** dictate that there must be some protons in the $\{Nb_{24}O_{72}\}$ and $\{Nb_{32}O_{96}\}$ clusters (i.e., $[Nb_{24}O_{72}H_{21}]^{3-}$, $[Nb_{32}O_{96}H_{28}]^{4-}$). As stated by Nyman and Niu, the very high number of crystallographically independent atoms and variable parameters prevented the direct location of the protons from the Fourier maps; even bond-valence calculations did not provide an obvious solution, as a result of atypical distortions and the relatively wide variation of the Nb−O bond length.[15] In the structures of the $\{Nb_{24}O_{72}\}$ and $\{Nb_{32}O_{96}\}$ units in compounds **1**−**3**, some long Nb−O_t bonds of the NbO_6 octahedra (shown in purple in Figure 1) linked to the $\{Nb_7O_{22}\}$ building blocks are in the range 2.347(7)−2.431(12) Å, and bond valence sum (BVS) calculations provided values of 0.311−0.405 for these Nb−O_t terminal oxygen atoms, indicating the most possible sites for protonation. The BVS values of the remaining terminal oxygen atoms in **1**−**3** are in the ranges 1.425−1.609, 0.893−1.533, and 1.387−1.689, respectively, suggesting that some terminal oxygen atoms can be monoprotonated. Thus, we think these protons would be localized or delocalized in polyniobate anion units on the basis of the previous studies by Nyman and Niu and the BVS calculations.[15]

Electrospray Ionization Mass Spectrometry of 1−3. Due to the high solubility of these compounds, we also investigated their solution chemistry via ESI-MS (electrospray ionization mass spectrometry) to determine what species are present when the pure, crystalline polyanionic salts are dissolved in water (Figure S9 and Table S2, Supporting Information). For **1**, we found that the $\{Nb_{24}O_{72}\}$ cluster associated with K^+, Na^+, and H^+ ions dominated the solution of pure, redissolved **1**. For **2**, $\{Nb_{32}O_{96}\}$ fragments also associated with K^+, Na^+, and H^+ cations in the 5−, 6−, or 7− charge state

were found, while for **3**, we found that the $\{Nb_{24}O_{72}\}$ fragments and $\{K_{12}Nb_{96}O_{288}\}$ clusters with associated K^+, Na^+, and H^+ ions dominated the solution of pure, redissolved **3**.

UV−Vis Diffuse Reflectance Spectra of 1−3. For the sake of studying the conductivity of **1**−**3**, the UV−vis diffuse reflectance spectra of their powder samples were measured to achieve their band gaps (E_g), which were determined as the intersection point between the energy axis and the line extrapolated from the linear portion of the adsorption edge in a plot of Kubelka−Munk function F against E.[19] As shown in Figures S10−S12 (Supporting Information), the corresponding well-defined optical absorption associated with E_g can be assessed at 3.35, 3.17, and 3.34 eV for compounds **1**−**3**, respectively, which reveals the presence of an optical band gap and the nature of semiconductivity. Their band gaps are comparable with those of reported niobate photocatalysts (3.3−3.5 eV) but are lower than that of $KTaO_3$ (3.82 eV, Figure S13 (Supporting Information)), known as one of the best inorganic materials for photochemical splitting of water.[12]

Photocatalytic Properties. In the photocatalytic system, we use samples **1**−**3** as the UV light photosensitizer and catalyst, $Co^{III}(dmgH)_2pyCl$ complex as H_2 evolution cocatalyst, and TEA as the sacrificial electron donor. It is well-known that some factors, such as the concentrations of TEA, sample, and cobaloximes, the amount of the solvents, and the content of water in the solvent, will greatly influence the performance of the catalyst system. Studies on the effect of solvents were made at a concentration of 100 mg of **1**−**3**, 100.1 mg of cobaloximes, and 10 mL of TEA. The optimum conditions for H_2 evolution were based on TEA (0.72 mM) in 90 mL of water (9/1 v/v). More or less TEA content in the water solution may result in a decrease of H_2 evolution.

To explore the photocatalytic H_2 evolution activities of **1**−**3**, 100 mg of sample **1**−**3** and 100.1 mg (0.25 mmol) of cobaloximes were dissolved in 100 mL of 10% TEA solution in a quartz cell. The catalyst solution was irradiated under UV irradiation using a 500 W mercury lamp. As shown in Figure 4a, for compound **1**, the H_2 evolution rates in three runs were 5161.4, 5233.5, and 5186.7 μmol h^{-1} g^{-1}, respectively. The total evolved H_2 during 12 h was 6232.7 μmol. However, for compound **2**, the H_2 evolution rates in three runs were 5312.5, 5032.5, and 4824.3 μmol h^{-1} g^{-1} and the total H_2 evolved over 12 h was 6069.6 μmol (Figure 4b). As shown in Figure 4c, for compound **3**, the H_2 evolution rates in three runs were 4804.1, 4802.3, and 4537.7 μmol h^{-1} g^{-1}, respectively, and the total evolved H_2 during 12 h was 5657.6 μmol. When these photocatalysts were kept at room temperature for a long time, we measured the UV−vis spectra of them at different times; as shown in Figures S14−S16 (Supporting Information), there were no significant changes in the UV−vis spectra of these photocatalysts, which show that these catalysts are stable in air. At the same time, the UV−vis spectra of these photocatalysts were not significantly changed after photocatalytic reaction, suggesting that these photocatalysts are stable under the performance of the catalyst system (Figures S17−S19, (Supporting Information)).

With Pt as the cocatalyst, the photocatalytic H_2 evolution activities of **2** and **3** were studied. A 100 mg amount of sample **2** or **3** and 100 mg of H_2PtCl_6 were dissolved in 100 mL of 10% TEA solution in a quartz cell. As shown in Figure S20 (Supporting Information), for compound **2**, the H_2 evolution rates in three runs were 5569.4, 4750.1, and 5415.9 μmol h^{-1} g^{-1}, respectively. The total evolved H_2 during 12 h was 6708.1

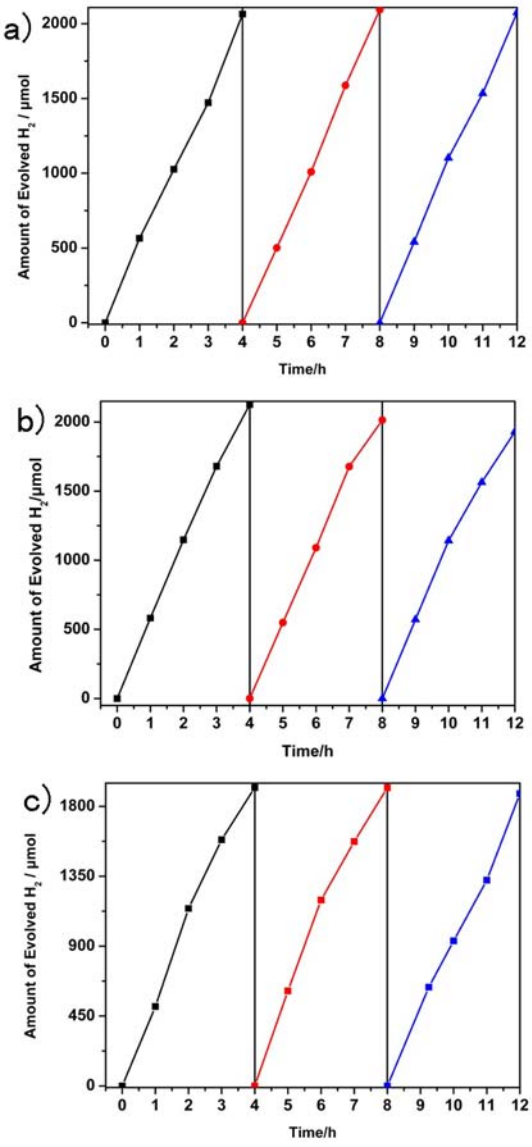

Figure 4. Time course of H_2 evolution from **1** (a), **2** (b), and **3** (c) and cobaloximes dissolved in 100 mL of 10% TEA solution under UV irradiation using a 500 W mercury lamp.

μmol. However, the H_2 evolution rates in three runs for compound **3** were 3974.7, 3930.9, and 3855.1 μmol h^{-1} g^{-1} and the total H_2 evolved over 12 h was 4704.2 μmol (Figure S21, Supporting Information).

To investigate the important role of **1**−**3** in the photocatalytic reactions, more experiments with different combinations were performed. Lines a (**1**), b (**2**), and c (**3**) in Figure 5 are derived from the first run of data of Figure 4. When cobaloximes are absent, the H_2 evolution rates of samples **1**−**3** were 3190.89, 4279.80, and 1654.27 μmol h^{-1} g^{-1}, respectively (lines d−f of Figure 5). As shown in Figure 5, no H_2 is detected when TEA is absent, suggesting that if the oxidation half-reaction does not work, the reduction half-reaction also does not work (line g of Figure 5). When **1**−**3** are absent (line h of Figure 5), cobaloxime alone shows no photocatalytic activity, indicating that **1**−**3** play a crucial role in light harvesting for photocatalysis.

In order to compare the photocatalytic activity of these compounds with that of related condensed solids, $KTaO_3$ was

dx.doi.org/10.1021/ja303723u | J. Am. Chem. Soc. 2012, 134, 14004−14010

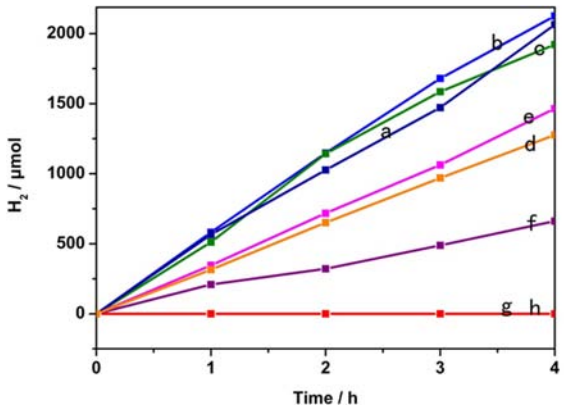

Figure 5. Time courses of photocatalytic H_2 evolution over different photocatalytic systems: (a–c) **1–3** as photocatalysts; (d–f) the absence of cobaloximes; (g) the absence of TEA; (h) the absence of **1–3**.

chosen to investigate its photocatalytic H_2 evolution activity under the same experimental conditions. As shown in Figure S22a (Supporting Information), the H_2 evolution rate of $KTaO_3$ with cobaloximes as the cocatalyst was 5051.8 μmol h^{-1} g^{-1}. However, with H_2PtCl_6 as cocatalyst, the H_2 evolution rate was 4984.4 μmol h^{-1} g^{-1} (Figure S22b). When cocatalyst is absent, the H_2 evolution rate of $KTaO_3$ was 4197.2 μmol h^{-1} g^{-1} (Figure S22c). One point is worth paying attention to: the PONbs herein are homogeneous (soluble) and $KTaO_3$ is heterogeneous. Although homogeneous catalysis has advantages in activity and selectivity over heterogeneous catalysis, it can be seen that the UV light photocatalytic H_2 evolution activities of these compounds are inferior to that of $KTaO_3$ on the whole. A summary of the photocatalytic experiments is given in Table S3 (Supporting Information).

CONCLUSION

In summary, we have synthesized and structurally characterized the three nanosized high-nuclearity polyoxoniobates **1–3**, which are based on $[Nb_7O_{22}]^{9-}$ subunits. Compound **1** is the first isolated inorganic isopolyoxoniobate $\{Nb_{24}O_{72}\}$. Compound **2** possesses a unique molecular square shape $\{Nb_{32}O_{96}\}$ cluster, representing the largest isopolyoxoniobate cluster reported so far. Compound **3** is an unprecedented cuboctahedral molecular cage $\{K_{12}Nb_{96}O_{288}\}$ constructed from a triangular "bowl-shaped" $\{Nb_{24}O_{72}\}$ SBU, which is the largest solid aggregation of polyoxoniobate. Moreover, the photocatalytic H_2 evolution activities of compounds **1–3** have been investigated under UV light irradiations. The discovery of these new polyoxoniobate clusters affords new opportunities for developing polyoxoniobate chemistry and exploring highly efficient photocatalysts. We will put more effort into the applicability of this synthetic strategy so as to provide general insights into polyoxoniobate synthesis.

ASSOCIATED CONTENT

Supporting Information

Text, figures, tables, and CIF files giving additional structural figures, XRPD, TGA, UV, ESI-MS, and UV–vis diffuse reflectance spectra, crystallographic data, and details of photocatalytic experiments. This material is available free of charge via the Internet at http://pubs.acs.org.

AUTHOR INFORMATION

Corresponding Author

*zmsu@nenu.edu.cn; wangxl824@nenu.edu.cn; wangeb889@nenu.edu.cn

Notes

The authors declare no competing financial interest.

ACKNOWLEDGMENTS

We gratefully acknowledge financial support from the NNSF of China (Nos. 21001022, 21171033, 21131001), the NGFR 973 Program of China (No. 2010CB635114), NCET in Chinese University (No. NCET-10-0282), PhD Station Foundation of Ministry of Education (No. 20100043110003), the FANEDD of the People's Republic of China (No. 201022), the STDP of Jilin Province (Nos. 201001169, 20111803), and the FRFCU (Nos. 09ZDQD003, 10CXTD001).

REFERENCES

(1) (a) Long, D. L.; Burkholder, E.; Cronin, L. *Chem. Soc. Rev.* **2007**, *36*, 105–121. (b) Rhule, J. T.; Hill, C. L.; Judd, D. A. *Chem. Rev.* **1998**, *98*, 327–357. (c) Mizuno, N.; Misono, M. *Chem. Rev.* **1998**, *98*, 199–217. (d) Pope, M. T.; Müller, A. *Angew. Chem., Int. Ed.* **1991**, *30*, 34–48.

(2) (a) Müller, A.; Krickemeyer, E.; Bögge, H.; Schmidtmann, M.; Beugholt, C.; Kögerler, P.; Lu, C. *Angew. Chem., Int. Ed.* **1998**, *37*, 1220–1223. (b) Müller, A.; Shah, S. Q. N.; Bögge, H.; Schmidtman, M. *Nature* **1999**, *397*, 48–50. (c) Müller, A.; Kögerler, P.; Dress, A. W. M. *Coord. Chem. Rev.* **2001**, *222*, 193–218. (d) Botar, B.; Kögerler, P.; Hill, C. L. *J. Am. Chem. Soc.* **2006**, *128*, 5336–5337.

(3) (a) Klemperer, W. G.; Marquart, T. A.; Yaghi, O. M. *Angew. Chem., Int. Ed.* **1992**, *31*, 49–51. (b) Kortz, U.; Müller, A.; van Slageren, J.; Schnack, J.; Dalal, N. S.; Dressel, M. *Coord. Chem. Rev.* **2009**, *253*, 2315–2327. (c) Müller, A.; Peters, F.; Pope, M. T.; Gatteschi, D. *Chem. Rev.* **1998**, *98*, 239–272. (d) Yamase, T. *Chem. Rev.* **1998**, *98*, 307–325. (e) An, H. Y.; Wang, E. B.; Xiao, D. R.; Li, Y. G.; Su, Z. M.; Xu, L. *Angew. Chem., Int. Ed.* **2006**, *45*, 904–908. (f) Zheng, S. T.; Zhang, H.; Yang, G. Y. *Angew. Chem., Int. Ed.* **2008**, *47*, 3909–3913.

(4) (a) Cjoamg, M. H.; Williams, C. W.; Soderhlm, L.; Antonio, M. R. *Eur. J. Inorg. Chem.* **2003**, *14*, 2663–2669. (b) Russell, A. J.; Berberich, J. A.; Drevon, G. F.; Koepsel, R. R. *Annu. Rev. Biomed. Eng.* **2003**, *5*, 1–27. (c) Kortz, U.; Savelieff, M. G.; Bassil, B. S.; Keita, B.; Nadjo, L. *Inorg. Chem.* **2002**, *41*, 783–789. (d) Besserguenew, A.; Dickman, M.; Pope, M. *Inorg. Chem.* **2001**, *40*, 2582–2586. (e) Ohlin, C. A.; Villa, E. M.; Fettinger, J. C.; Casey, W. H. *Angew. Chem., Int. Ed.* **2008**, *47*, 5634–5636. (f) Nyman, M. *Dalton Trans.* **2011**, *40*, 8049–8058. (g) Huang, P.; Qin, C.; Wang, X. L.; Sun, C. Y.; Yang, G. S.; Shao, K. Z.; Jiao, Y. Q.; Zhou, K.; Su, Z. M. *Chem. Commum.* **2012**, *48*, 103–105.

(5) (a) Wassermann, K.; Dickman, M. H.; Pope, M. T. *Angew. Chem., Int. Ed.* **1997**, *36*, 1445–1448. (b) Müller, A. P.; Kuhlmann, K. C. *Chem. Commun.* **1999**, *15*, 1347–1358. (c) Lindqvist, I. *Ark. Kemi* **1953**, *5*, 247–250.

(6) Graeber, E. J.; Morosin, B. *Acta Crystallogr.* **1977**, *B33*, 2137–2143.

(7) Nyman, M.; Bonhomme, F.; Alam, T. M.; Rodriguez, M. A.; Cherry, B. R.; Krumhansl, J. L.; Nenoff, T. M.; Sattler, A. M. *Science* **2002**, *297*, 996–998.

(8) (a) Nyman, M.; Bonhomme, F.; Alam, T. M.; Parise, J. B.; Vaughan, G. M. B. *Angew. Chem., Int. Ed.* **2004**, *43*, 2787–2792. (b) Bonhomme, F.; Larentzos, J. P.; Alam, T. M.; Maginn, E. J.; Nyman, M. *Inorg. Chem.* **2005**, *44*, 1774–1785. (c) Hou, Y.; Nyman, M.; Rodriguez, M. A. *Angew. Chem., Int. Ed.* **2011**, *50*, 12514–12517.

(9) Maekawa, M.; Ozawa, Y.; Yagasaki, A. *Inorg. Chem.* **2006**, *45*, 9608–9609.

(10) Tsunashima, R.; Long, D. L.; Miras, H. N.; Gabb, D.; Pradeep, C. P.; Cronin, L. *Angew. Chem., Int. Ed.* **2010**, *49*, 113–116.

(11) (a) Yamase, T.; Watanabe, R. *J. Chem. Soc., Dalton Trans.* **1986**, *8*, 1669. (b) Akid, R.; Darwent, J. R. *J. Chem. Soc., Dalton Trans.* **1985**, *2*, 395−399. (c) Darwent, J. R. *J. Chem. Soc., Chem. Commun.* **1982**, *14*, 798−799. (d) Hill, C. L.; Bouchard, D. A. *J. Am. Chem. Soc.* **1985**, *107*, 5148−5157. (e) Ioannidis, A.; Papaconstantinou, E. *Inorg. Chem.* **1985**, *24*, 439−441. (f) Dang, L. Q.; You, W. S.; Zhang, X.; Huang, C. Y.; Lei, Z. B.; Sun, Z. G.; Li, C. *Chin. Chem. Lett.* **2006**, *17*, 973−976. (g) Yamase, T. *Inorg. Chim. Acta* **1982**, *64*, L155. (h) Yamase, T. *Inorg. Chim. Acta* **1983**, *76*, L25−L27. (i) Yamase, T.; Takabayashi, N.; Kaji, M. *J. Chem. Soc., Dalton Trans.* **1984**, *5*, 793−799. (j) Yamase, T.; Cao, X. O.; Yazaki, S. *J. Mol. Catal. A: Chem.* **2007**, *262*, 119−127. (k) Geletii, Y. V.; Huang, Z. Q.; Hou, Y.; Musaev, D. G.; Lian, T. Q.; Hill, C. L. *J. Am. Chem. Soc.* **2009**, *131*, 7522−7523. (l) Yin, Q. S.; Tan, J. M.; Besson, C.; Geletii, Y. V.; Musaev, D. G.; Kuznetsov, A. E.; Luo, Z.; Hardcastle, K. I.; Hill, C. L. *Science* **2010**, *328*, 342−345.

(12) Osterloh, F. E. *Chem. Mater.* **2008**, *20*, 35−54.

(13) Zhang, Z.; Lin, Q.; Kurunthu, D.; Wu, T.; Zuo, F.; Zheng, S. T.; Bardeen, C. J.; Bu, X.; Feng, P. Y. *J. Am. Chem. Soc.* **2011**, *133*, 6934−6937.

(14) Goiffon, A.; Philippot, E.; Maurin, M. *Rev. Chim. Miner.* **1980**, *17*, 466−476.

(15) (a) Bontchev, R. P.; Nyman, M. *Angew. Chem., Int. Ed.* **2006**, *45*, 6670−6672. (b) Niu, J. Y.; Ma, P. T.; Niu, H. Y.; Li, J.; Zhao, J. W.; Song, Y.; Wang, J. P. *Chem. Eur. J.* **2007**, *13*, 8739−8748.

(16) (a) Filowitz, M.; Ho, R. K. C.; Klemperer, W. G.; Shum, W. *Inorg. Chem.* **1979**, *18*, 93−103. (b) Wen, F. Y.; Yang, J. H.; Zong, X.; Ma, B. J.; Wang, D. G.; Li, C. *J. Catal.* **2011**, *281*, 318−324.

(17) Sheldrick, G. M. *SHELXL-97, Program for the Refinement of Crystal Structure*; University of Göttingen, Göttingen, Germany, 1997.

(18) Spek, A. L. *PLATON, A Multipurpose Crystallographic Tool*; Utrecht University, Utrecht, The Netherlands, 2003.

(19) Pankove, J. I. *Optical Processes in Semiconductors*; Prentice-Hall: Englewood Cliffs, NJ, 1971; p 34.